

**RESONANT ELASTIC SCATTERING AND ELECTRON  
CAPTURE BY Al-LIKE P<sup>2+</sup> AND S<sup>3+</sup> IONS  
AT LOW ENERGIES**

**Abdulrahman Al-Mulhem, Abdelkarim Mekki, and**

**Ibraheem Nasser\***

*Department of Physics  
King Fahd University of Petroleum & Minerals  
Dhahran, Saudi Arabia*

الخلاصة :

تَمَّ حساب المقاطع المستعرضة ومعاملات المعدلات لكل من الالتقاط الإلكتروني الرنيني والتشتت المرن الرنيني للأيونات الشبيهة بالألمنيوم عند الطاقات المنخفضة . وقد تَمَّ بالتفصيل حساب معدلات الإنبعاث الإشعاعي وانبعاث (أوجيه) للإلكترونات الخاصة بالمدارات الإنتقالية المنخفضة . وتَمَّ بالقياس استعمال الحسابات للمدارات الإنتقالية العالية . لقد أُستُخدم في الحسابات الإقتران الزاوي المغزلي مع استخدام الدوال غير النسبية المسماة (هارتري فوك) وأُخذ متوسط المقاطع لمقدار من الطاقة (٠,٠١) رايدبرغ . ووُجد أن المساحات المستعرضة للتشتت المرن الرنيني أكبر من المساحات المستعرضة للإلتقاط الإلكتروني الرنيني بقيم تتراوح بين (١٠٠٠٠٠ - ١٠٠٠٠٠٠) ووُجد أن هذه القيم تتناقص مع زيادة العدد الذري للأيونات التي تنتمي لسلسلة الألمنيوم والمتفقة في عدد الإلكترونات .

\*Address for correspondence:  
KFUPM Box No. 1994  
King Fahd University of Petroleum & Minerals  
Dhahran 31261  
Saudi Arabia

## **ABSTRACT**

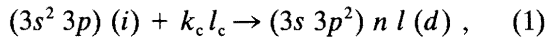
Resonant electron capture and elastic scattering cross sections and rate coefficients of the ground state  $(3s^2 3p)^2 P$  of Al-like  $P^{2+}$  and  $S^{3+}$  are calculated at low energies ( $e_c < 0.65$  Ry). Explicit calculation of Auger and radiative transition probabilities are evaluated at low  $n$  ( $n < 11$ ), and extrapolated to high  $n$ -values. These probabilities were calculated using single configuration non-relativistic Hartree–Fock wavefunctions in LS coupling. We averaged the cross sections over an energy bin of width  $\Delta e_c = 0.01$  Ry. The resonance elastic scattering cross sections are 4 to 6 orders of magnitude larger than the capture cross sections, mainly because of the smallness of the fluorescence yields of the resonance levels. The resonance elastic scattering cross sections are found to decrease with increasing the atomic number in a given isoelectronic sequence.

## RESONANT ELASTIC SCATTERING AND ELECTRON CAPTURE BY AI-LIKE P<sup>2+</sup> AND S<sup>3+</sup> IONS AT LOW ENERGIES

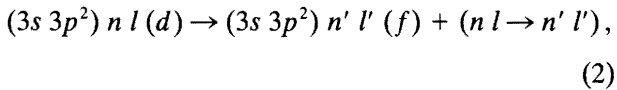
### 1. INTRODUCTION

Resonance excitation, which combines both resonant excitation and resonant elastic scattering, is the complementary process to dielectronic recombination, and the latter is of major importance in radiation cooling of high-temperature plasmas. The probabilities of these processes are related by [1]  $P_{DR} + P_{RE} = 1$ . In order to make a precise description of the behavior of such plasmas, accurate estimation of the DR, RE, and other processes rate coefficients for many different ions is needed.

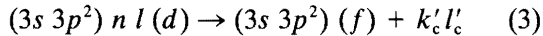
The dielectronic recombination process involves an initial excitation capture in going from an initial state  $i$  to one of the intermediate states  $d$ , such as



this is followed by a radiative decay of the intermediate state  $d$  to a final state  $f$ ,



while in the resonance excitation, the initial process is followed by emission of an Auger electron,



(Explicit reference to the core electrons of Al-like ions is omitted for simplicity).

In this paper we investigate the intermediate metastable series for Al-like ions such as  $(3s 3p^2)^4 P n l$  which are close to the ground state  $(3s^2 3p)^2 P$ . The processes treated in this paper are relatively simple mainly because (i) there is only one Auger channel  $(3s 3p^2 n l \rightarrow 3s^2 3p k_c l_c)$ , and (ii) the radiative transition probabilities ( $A_r$ ) are dependent on the outer electron due to the forbidden transition of the core, this means that high Rydberg states contribution ( $n > 30$ ) are small and negligible because of the well known scaling of  $A_r$ ,  $A_r \propto 1/n^3$ .

In Section 2 we briefly summarize the theoretical procedure employed in the evaluation of the DR and RES cross sections and rate coefficients. In Section 3 we present the results of our data, followed by a conclusion in Section 4.

### 2. THEORETICAL PROCEDURE

The details of the theoretical procedure used in the present work are covered in full in previous publication by Hahn, and Hahn and LaGattuta [2, 3]. Therefore, only a brief summary of the main assumptions is presented.

We define an energy-averaged [4] cross section  $\bar{\sigma}^{DR}$ , and  $\bar{\sigma}^{RES}$

$$\bar{\sigma}^{DR} \equiv \frac{1}{\Delta e_c} \int_{e_c - \frac{\Delta e_c}{2}}^{e_c + \frac{\Delta e_c}{2}} \sigma^{DR}(e') de', \quad (4)$$

$$\bar{\sigma}^{RES} \equiv \frac{1}{\Delta e_c} \int_{e_c - \frac{\Delta e_c}{2}}^{e_c + \frac{\Delta e_c}{2}} \sigma^{RES}(e') de', \quad (5)$$

$$\sigma^{DR} = \frac{4\pi(\text{Ry})}{e_c(\text{Ry})} \tau_0 V_a(i \rightarrow d) \omega(d) \frac{1}{\Delta e_c} (\pi a_0^2), \quad (6)$$

$$\sigma^{RES} = \frac{4\pi(\text{Ry})}{e_c(\text{Ry})} \tau_0 V_a(i \rightarrow d) Z(d) \frac{1}{\Delta e_c} (\pi a_0^2), \quad (7)$$

where  $V_a$  is the radiationless excitation capture probability which is related, by detailed balance [5], to the Auger emission probability  $A_a(d \rightarrow i)$  by  $V_a = (g_d/2g_i) A_a(d \rightarrow i)$ , where  $g_d$  and  $g_i$  are statistical weights of the intermediate and initial states, respectively. Here  $a_0$  and  $\tau_0$  are the Bohr radius and atomic unit of time.  $e_c$  is the energy of the incident electron, and  $\Delta e_c$  is a small energy bin which is chosen arbitrary but with the requirement that it is small compared with the actual experimental continuum electron beam width.  $Z(d) = A_a(d \rightarrow i)/\Gamma(d)$  and  $\omega(d \rightarrow f) = A_r(d \rightarrow f)/\Gamma(d)$  are the partial Auger and fluorescence yields of the state  $d$ , respectively.  $A_r$  is the radiative transition probability.  $\Gamma(d) = \sum_i A_a(d \rightarrow i) + \sum_f A_r(d \rightarrow f)$  is the total width of the intermediate state. In general, the rates  $\bar{\alpha}^{DR}$ , and  $\bar{\alpha}^{RES}$  are given by [4],

$$\bar{\alpha}^{DR} = \left( \frac{4\pi(\text{Ry})}{kT(\text{Ry})} \right)^{3/2} a_0^3 V_a(i \rightarrow d) \omega(d) \exp(-e_c/kT), \quad (8)$$

$$\bar{\alpha}^{RES} = \left( \frac{4\pi(\text{Ry})}{kT(\text{Ry})} \right)^{3/2} a_0^3 V_a(i \rightarrow d) Z(d) \exp(-e_c/kT). \quad (9)$$

In general, the cross sections  $\bar{\sigma}^{\text{DR}}$ ,  $\bar{\sigma}^{\text{RES}}$  and the rates  $\bar{\alpha}^{\text{DR}}$ ,  $\bar{\alpha}^{\text{RES}}$  are related by [3]:

$$\bar{\sigma}^{\text{DR}} = (4.06 \times 10^{-9}) \frac{kT}{(\text{Ry})^{3/2}} \frac{\exp(e_c/kT)}{e_c \Delta e_c} \bar{\alpha}^{\text{DR}}, \quad (10)$$

$$\bar{\sigma}^{\text{RES}} = (4.06 \times 10^{-9}) \frac{kT}{(\text{Ry})^{3/2}} \frac{\exp(e_c/kT)}{e_c \Delta e_c} \bar{\alpha}^{\text{RES}}. \quad (11)$$

Cowan's code, in single-configuration Hartree-Fock approximation and in full LS coupling, was used in the calculation of the transition energies as well as the relevant  $A_a$  and  $A_r$  needed in the evaluation of the DR and RES cross sections. Data tables [6] were used to adjust energies, wherever possible. This is important, especially when the transition energies are small. Cowan's code was used to evaluate energy levels for all intermediate states with  $n < 10$ . Auger transition probabilities,  $A_a$  require both bound and continuum wavefunctions. The continuum wavefunctions were generated [2, 3] by a distorted-wave method using the Hartree-Fock potential.

**Table 1. Values of  $\bar{\sigma}^{\text{DR}}$  and  $\bar{\sigma}^{\text{RES}}$  in Units of  $\text{cm}^2$  versus  $e_c(\text{Ry})$  for the Intermediate Metastable Series  $(3s 3p^2)^4 P n l$  of  $\text{P}^{2+}$ ,  $\Delta e_c = 0.01 \text{ Ry}$ . Powers of 10 are shown in Parenthesis.**

$e_c(\text{Ry})$	$\bar{\sigma}^{\text{DR}} (\text{cm}^2)$	$\bar{\sigma}^{\text{RES}} (\text{cm}^2)$
0.01	3.20(-20)	5.98(-14)
0.19	3.45(-21)	1.44(-15)
0.21	1.36(-20)	1.51(-15)
0.24	1.13(-21)	1.25(-15)
0.26	1.82(-28)	1.86(-17)
0.32	1.02(-21)	3.58(-16)
0.33	3.05(-21)	5.08(-16)
0.34	4.55(-22)	4.05(-16)
0.35	4.87(-29)	1.13(-17)
0.38	5.57(-22)	1.54(-16)
0.39	1.49(-21)	2.40(-16)
0.40	2.49(-22)	1.97(-16)
0.42	1.19(-21)	2.17(-16)
0.43	1.55(-22)	1.11(-16)
0.44	9.24(-22)	1.69(-16)
0.45	4.36(-22)	2.00(-16)
0.46	8.81(-22)	1.84(-16)
0.47	6.09(-22)	1.45(-16)
0.48	5.50(-22)	1.36(-16)
0.49	3.62(-22)	6.58(-17)
0.50	1.05(-22)	1.67(-17)
Total	6.22(-20)	6.71(-14)

### 3. RESULTS AND DISCUSSION

DR and RES cross sections and rate coefficients for Al-like  $\text{P}^{2+}$  and  $\text{S}^{3+}$  for the intermediate metastable state series  $(3s 3p^2)^4 P n l$  were evaluated in LS coupling. The cross sections  $\bar{\sigma}^{\text{DR}}$  and  $\bar{\sigma}^{\text{RES}}$  in units of  $\text{cm}^2$  for  $\text{P}^{2+}$  are given in Table 1 as a function of  $e_c(\text{Ry})$ . As shown in Table 1,  $\bar{\sigma}^{\text{RES}}$  are greater than  $\bar{\sigma}^{\text{DR}}$  by a factor of  $10^6$ . For  $\text{S}^{3+}$  ion, the cross sections  $\bar{\sigma}^{\text{DR}}(\text{cm}^2)$  and  $\bar{\sigma}^{\text{RES}}(\text{cm}^2)$  are tabulated in Table 2, the  $\bar{\sigma}^{\text{RES}}$  is still larger than  $\bar{\sigma}^{\text{DR}}$  by a factor of  $10^4$ . In Figures 1 and 2, the  $\log_{10}$  of the rate coefficients in

**Table 2. Values of  $\bar{\sigma}^{\text{DR}}$  and  $\bar{\sigma}^{\text{RES}}$  in Units of  $\text{cm}^2$  versus  $e_c(\text{Ry})$  for the Intermediate Metastable Series  $(3s 3p^2)^4 P n l$  of  $\text{S}^{3+}$ ,  $\Delta e_c = 0.01 \text{ Ry}$ . Powers of 10 are shown in Parenthesis.**

$e_c(\text{Ry})$	$\bar{\sigma}^{\text{DR}} (\text{cm}^2)$	$\bar{\sigma}^{\text{RES}} (\text{cm}^2)$
0.06	1.96(-19)	1.95(-16)
0.10	1.73(-20)	2.43(-15)
0.23	2.96(-21)	7.86(-16)
0.25	4.71(-21)	5.05(-16)
0.28	2.87(-20)	3.86(-17)
0.30	3.33(-21)	3.76(-16)
0.37	5.28(-22)	2.58(-16)
0.38	1.87(-21)	1.75(-16)
0.39	1.23(-20)	1.97(-17)
0.40	1.51(-21)	1.49(-16)
0.44	4.41(-25)	1.24(-16)
0.45	1.05(-21)	8.61(-17)
0.46	6.72(-21)	1.18(-17)
0.47	8.72(-22)	7.82(-17)
0.49	2.67(-25)	7.08(-17)
0.50	4.77(-21)	5.89(-17)
0.51	1.03(-21)	8.21(-17)
0.52	3.94(-22)	3.28(-17)
0.53	3.07(-21)	7.58(-17)
0.54	5.45(-22)	7.47(-17)
0.55	2.49(-21)	7.16(-17)
0.56	1.93(-21)	4.51(-17)
0.57	1.38(-21)	4.47(-17)
0.58	1.24(-21)	5.88(-17)
0.59	1.07(-21)	5.03(-17)
0.60	1.60(-21)	4.18(-17)
0.61	8.67(-22)	2.56(-17)
0.62	9.70(-22)	1.71(-17)
0.63	9.54(-22)	7.53(-18)
0.64	6.49(-23)	1.27(-19)
Total	3.01(-19)	5.99(-15)

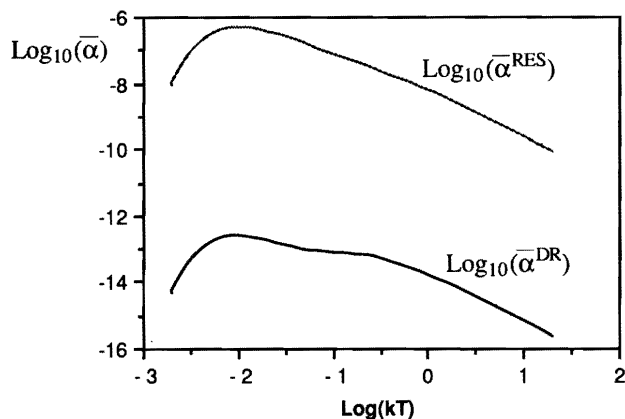


Figure 1.  $\text{Log}_{10} \bar{\alpha}^{DR}$  and  $\text{Log}_{10} \bar{\alpha}^{RES}$  in Units of  $\text{cm}^3/\text{s}$  as Functions of  $\text{Log}_{10} kT(\text{Ry})$  for  $\text{P}^{2+}$ .

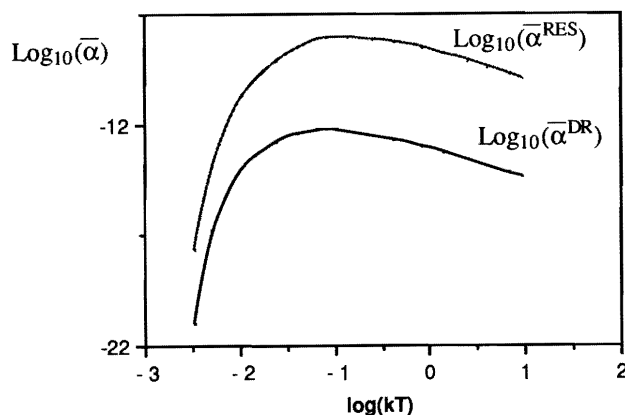


Figure 2.  $\text{Log}_{10} \bar{\alpha}^{DR}$  and  $\text{Log}_{10} \bar{\alpha}^{RES}$  in Units of  $\text{cm}^3/\text{s}$  as Functions of  $\text{Log}_{10} kT(\text{Ry})$  for  $\text{S}^{3+}$ .

units of ( $\text{cm}^3/\text{s}$ ) for  $\text{P}^{2+}$  and  $\text{S}^{3+}$  are plotted as a function of  $\text{log}_{10} kT(\text{Ry})$ . For  $\text{P}^{2+}$  the rates peak near  $kT = 0.001 \text{ Ry}$ , with the values  $0.25 \times 10^{-12} \text{ cm}^3/\text{s}$ , and  $0.48 \times 10^{-6} \text{ cm}^3/\text{s}$  for DR and RES, respectively. For  $\text{S}^{3+}$  the rates peak near  $kT = 0.01 \text{ Ry}$ , with the values  $0.82 \times 10^{-12} \text{ cm}^3/\text{s}$  and  $0.11 \times 10^{-7} \text{ cm}^3/\text{s}$  for DR and RES, respectively. The rate coefficients of  $\text{P}^{2+}$  decay much faster than those of  $\text{S}^{3+}$ . The sudden drop in the DR cross sections of  $\text{P}^{2+}$  at the

continuum energies  $e_c = 0.26$  and  $0.35 \text{ Ry}$ , are mainly due to the smallness of the radiative transitions probability of the intermediate states  $(3s 3p^2) 4f$  and  $(3s 3p^2) 5f$ , respectively.

Due to the unitary nature of the mixing matrix, the total cross sections are generally much less sensitive to the mixing (in order of  $\pm 10\%$  change), although the individual states are sometimes very much affected by it. The dependence of our results on the coupling scheme used is also very weak in so far as the total is concerned. That is why we neglected these and other possible complications in the present calculations.

#### 4. CONCLUSION

We have calculated DR and RES cross sections and rate coefficients for the intermediate metastable state series  $(3s 3p^2)^4 P n l$  of Al-like  $\text{P}^{2+}$  and  $\text{S}^{3+}$ . Explicit cross sections are listed in Tables 1 and 2 as a function of  $e_c(\text{Ry})$ . Figures 1 and 2 display  $\text{log}_{10}$  of the rate coefficients as a functions of  $\text{log}_{10} kT(\text{Ry})$ . The RES are larger than DR by an order of magnitude [4–6]. DR cross sections and rates increase with increasing atomic number in a given isoelectronic sequence; unlike in DR, the RES cross sections and rates decrease with increasing atomic number in a given isoelectronic sequence. Similar work for DR and RE is in progress to study the main behavior of the cross sections and rates for different ions in the Al-like sequence.

#### ACKNOWLEDGEMENTS

This work was carried out at KFUPM computer center using Cowan's atomic structure code.

#### REFERENCES

- [1] G. Omar and Y. Hahn, *Phys. Rev. A*, **37** (1988), p. 1983.
- [2] Y. Hahn, *Adv. At. Mol. Phys.*, **21** (1985), p. 123.
- [3] Y. Hahn and K. LaGattuta, *Phys. Rep.*, **166** (1988), p. 195.
- [4] I. Nasser, *Arabian Journal for Science & Engineering*, **16(1)** (1991), p. 85.
- [5] P. F. Dittner, S. Datz, R. Hippler, H. F. Krause, P. D. Miller, P. L. Pepmiller, C. M. Fou, Y. Hahn, and I. Nasser, *Phys. Rev. A*, **38** (1988), p.2762.
- [6] S. Bashkin and J. O. Stoner, Jr., *Atomic Energy Levels and Grotrian Diagrams*. Amsterdam: North-Holland, 1977.

Paper Received 28 December 1991; Revised 25 March 1992.